GEM TN-93-302

The Axial+Projective Alignment for Muon Chambers

A. Korytov
Massachusetts Institute of Technology

February 18, 1993

Abstract:

Proposed is a possible realization of an axial alignment technique, based on a stretched wire with the mini-strip readout. The advantage of the axial alignment is combination with the projective one is discussed and the merits of the proposed scheme are presented.

February 18, 1993
A.Korytov,
MIT

The Axial+Projective Alignment for Muon Chambers.

Summary.

Proposed is a possible realization of an axial alignment technique, based on a stretched wire with the mini-strip readout. The advantage of the axial alignment in combination with the projective one is discussed and the merits of the proposed scheme are presented.

1. Introduction.

The idea of projective alignment was proposed by G.Mitselmakher and A.Ostapchuk [1]. This approach allows one to relax requirements on chamber placement and makes it possible to correct different kinds of misalignment (shifts, rotations, expansion, torque and etc.) with a limited number of alignment paths by making use of the interpolation technique.

In the current CSC design [2] with a limited length and width of chambers there are many towers, which can be difficult to align in a projective way.

This would result in:

1) either gaps in coverage or sophisticated and unnatural chamber design with many holes;

2) complication, i.e. many different alignment fixtures must be fabricated at various inclinations in q and j, plus many projective alignment paths must be adjusted to point at the IP;

3) and maybe cost (many high accuracy and wide range alignment detectors are apparently not cheap).

The axial alignment in combination with the projective one (at $\theta=90^0$ and 30^0) was discussed in the LSDT version of the Muon System [3]. The real advantage of this is a simplification of overlapping chambers to make the coverage as full as possible. The price one would have to pay for this is that the interpolation procedure should be applied to an effectively "very long chamber" which actually consists of several individual chambers "tied" together with an axial alignment (fig.1). In fact the situation is much better than a "very long chamber". The notion of a "very long chamber" would be appropriate if one would tie the chambers by making use of proximity alignment detectors. However, the axial alignment gives a lot of information about the relative positions of the internal points with respect to the external ones where the projective paths go.

As shown by J.Paradiso [4] and A.Ostapchuk [5], "axial+projective" alignment is acceptable from the interpolation procedure point of view. What it results in is a requirement for the axial alignment to be of the order of half mil and maybe more strict tolerances on a chamber placement.

In the next section we will give an estimation of how big the coverage gaps would be if one would proceed with the projective alignment alone. Then, the possibility of a simple and elegant axial alignment technique with a wide range and high accuracy will be shown.

2. Why the axial alignment.

Fig.2(a,b) and Appendix 1 show how the coverage gaps could be calculated.

Fig.3 shows the geometry which has been used in the calculations.

The main assumptions were as follows:

1) Six gap strip chambers with one inch hexel planes were assumed everywhere, resulting in the total chamber thickness of 17.5 cm;
2) Strip chambers with 5 cm dead zone on edges were assumed;
3) The middle super layer was required to have 5 cm clearance between chambers for the support structures; both the first and the last super layer were free of this requirement;
4) Projective alignment lens was assumed to be 5 cm in diameter [6];
5) At least one hit per super layer was required;
6) Four projective towers in the barrel and two in the end-caps were assumed.

In case of the axial alignment, the optical clearance for the lens is not needed. This is the only difference (in terms of chamber layout) between the two schemes.

Table 1 and 2 summarize the difference in coverage. The gain of using axial alignment is obvious.

One can notice that once the "many-tower" projective alignment is given up, further optimization becomes possible: there is no need to have the projective chamber layout through out all super layers. In particular, the middle super layer could be split in three chambers instead of four (fig.4). This new layout:

1) Decreases even more the loss of coverage (table 3),
2) Saves number of chambers and channels and
3) Ensures that each track has hits in at least two super layers;
4) Also, all chambers in the barrel are now of the same length 3.5 m.

It should be mentioned here that the difference in coverage between the two alignment schemes (projective only and axial+projective) does not depend on the definition how many points per superlayer is required (Appendix 1). Thus, the axial alignment with the new layout is always ~4% more efficient than the old scheme.

Table 4 is given to stress the difference in coverage between the two schemes of alignment. The advantage of the axial+projective alignment is, for example, about 20% increase in the efficiency for detecting "4μ-naive" events.

Also, the axial alignment seems to give a considerable simplification of the support structures since it eliminates the interference of the support membranes going between chambers of the SL2 and the projective alignment paths [7].

In addition, the axial multipoint alignment scheme may have benefits for the global alignment of each sector [8].

Also, the axial monitoring of the chamber mid-points allows one to exclude such chamber deformations as a simple droop (this seems to be not correctable with the projective alignment alone) [9].

In the next section one will see that the last two merits can be trivially obtained with the particular alignment scheme to be discussed below.

3. A stretched wire and mini-strips.

Before going further, it is worthwhile mentioning the goal: typically a half mil accuracy in the transverse (r_φ) direction (i.e., much smaller in quadrature than 25 μm allowed for the overall alignment of super layers) over 10 mm range and a several times worse accuracy in radial direction over the same range.

There is a new and very elegant possible realization of an axial alignment which looks even more attractive when applied to CSC's. The idea is shown in fig.5. The strip boards are made with parts sticking out of the chambers. These parts contain bands of mini-strips (e.g., 25 mm long and 1 mm wide strips) which were etched with the readout strips*). It is these mini-strips that will provide the axial alignment. A wire stretched over these strips through the entire sector and carrying a low frequency signal will induce a charge on these strips. The centroid of the distribution indicates the left/right ("horizontal", or r_φ) position of the wire, while the width should allow calculating the wire height ("vertical", or radial position)**), -- fig.6(a,b). One can notice that this is not different from the way the position of an avalanche is read out from the regular strips.

The projective lines at the extremes in θ remain in the system. All inner chambers are tied together by the axial alignment which measures the position of the chambers in two directions (r_φ and radial). The two lines of two-dimensional measurements make possible distinguishing all kinds of inner chamber misalignments due to shifts, rotations, torque, expansion and so on. The longitudinal shifts (axial direction) are not measured, but they only need to be known with an accuracy of 1-2 cm.

Also, if additional alignment point are added between outer edges of chambers, one obviously gets the information about the chamber droop, or bend, i.e. the information which seems to not available from the projective alignment alone.

The wire (15 m long for the third super layer) will definitely droop. Regular tungsten wire would droop by less than 3 mm which is well within the range we are aiming for. To predict the sag of this wire with a 5 μm

---

*) Should it be necessary, the ministrips may be obviously etched on separate small boards and attached to chambers

**) The amplitude of the distribution is an additional information about the wire height.

precision, one would have to monitor the wire tension with a 10^{-3} accuracy which is still doable. However, there are other kinds of carbon wires [10]: e.g., a silicon carbide SCS-6 wire has 500 ksi minimum tensile strength and 3.0 g/cc density (compare to W: 450-590 ksi and 19.3 g/cc). This wire would droop by about 300 μm at a tension of 80% of tensile strength. Using wires of this kind***) relaxes the accuracy requirement for tension monitoring up to a few percent (~2%) which is trivial.

To understand what kind of accuracy we may expect from this method, we performed the calculations. However, before discussing results, let us make several other very important points.

If one wishes to construct a "high accuracy+wide range" alignment system such as the LED-LENS-QUAD one or a stretched wire between two planes with a capacitive readout, the most difficult thing would be a problem of systematic errors. The accuracy of 10 μm with 10 mm range means 10^{-3} accuracy in calibration. This kind of absolute calibration in many channels may be a state-of-the-art in many cases. This problem comes from the attempt to get the high accuracy in a wide range with essentially two readout devices.

In the case of mini-strips, the strip width is ~1 mm; and 10 times worse electronics with a 1% accuracy in calibration would result in the same 10 μm. And now the range is determined not by the calibration accuracy but by the number of mini-strips one would wish to have. (Notice that the bigger the number of strips, the better accuracy one gets due to effectively multiple measurements of the same value).

All kinds of random (from measurement to measurement) errors (such as thermal noise of electronics, pick-up noise, wire vibrations and etc.) are not a problem at all: there is no need to have 10 μm in each individual measurement. The random errors can be easily killed by statistics: by repeating the measurement, e.g., N times one easily reduces this contribution by a factor sqrt(N).

In addition, the contribution of systematic errors such as calibration ones can be also reduced. If one generates a sin-wave signal on a wire with a

***) Some of them are reasonably conductive. The available 5.6 mil SCS-6 wire had a resistance which would correspond to ~1 MΩ for a length of 15 m. This is good enough for the frequencies of 100 Hz we are assuming. In addition, these wires might be probably made more conductive (the simplest part of a solution is to make them thicker, the coating is also not excluded).

period T and the readout is not synchronized with this period, the measured charges for different measurements will be in different places of preamp+ADC range. Thus, all kinds of small systematic non-linearities of the preamp+ADC responses will be effectively equivalent to the random noise.

On the other hand, if a one percent accuracy in the calibration turns out to be trivial, one may chose to readout a signal induced on mini-strips at the same frequency as a wire signal is generated. This must give a considerable suppression of the noise contribution.

The electrostatic calculations give the induced charge density as follows (Cauchy distribution -- fig.6(b)):

$$\rho(x,y) = \frac{\partial^2 q}{\partial x \partial y} = 2U_0 \cdot \varepsilon_0 \cdot \frac{\ln\frac{H}{r_0} + \ln\left(2 - \frac{r_0}{H}\right)}{H} \cdot \frac{1}{1+\left(\frac{x}{H}\right)^2} \qquad (1)$$

where U_0 is a voltage on a wire; H is a height, the distance between the wire and the strip board; r_0 is a wire radius; x is a coordinate across strips and y - a coordinate along strips (and a wire). The typical charge on a central strip (assuming one inch long and 1 mm wide mini-strips) is to be of the order of 1 pC for a 10 V wire signal.

In the calculations the following parameters were used: the mini-strip band contained 31 strips of 25 mm length, strip pitch was 1 mm, strip width - 0.8 mm; the wire signal was U_0=10 V. As was mentioned above, the random noise is no issue so that the electronics noise was not put in the calculations. Preamp+ADC calibration accuracy was assumed to be 0.5% [11] and independent for different strips.

The induced charges on all strips were calculated. Then, they were spoiled by the imperfect system of preamps and ADC's. After that, "measured" charges were used for fitting. The deviation of obtained parameters ("horizontal" (x) and "vertical" (H) wire positions) from the original ones represented the systematic error for the particular case of x, H and a set of calibration errors. 300 different sets of calibration errors were generated to evaluate the RMS of the resulting systematic errors and this was done for different x and H.

Fig.7 presents the RMS of systematic errors in the "horizontal" direction (x). One can see that within 10 mm range in the "horizontal" and "vertical" directions a half mil accuracy is easily achievable. Fig.8 shows that the errors in the "vertical" direction (H) are better than 25 μm, i.e. much better than needed.

We also checked the consequence of cross-talks. The cross-talks should not shift the peak position of the distribution, just making it a bit wider. As expected, even 5% strip-to-strip cross-talks did not deteriorate the transverse resolution. whilst the change of the distribution width resulted in only 5-10 μm shift in determination of H.

A tilt of the wire with respect to the chamber in the horizontal direction also makes the distribution a little wider, but does not effect its centroid. So does the vertical tilt. However, the combination of the two could give some trouble since it results in skewing the shape of the distribution. First, when we had assumed 5 mrad inclination of the wire in both directions (essentially this is chamber placement tolerances; wire droop is much smaller than that even for the 3 mm sag), we did not see any errors exceeding fitting errors of ~1 μm. To dramatize the effect, we had to use 10 mrad and even 20 mrad inclinations. And even these angles did not give much trouble (fig.9).

The last question to be answered is how accurately these mini-strips could be etched. The results presented by K. Lau [12] show that the etching accuracy achieved over 0.5 m wide and 1 m long strip boards produced for the Houston CSC prototype is a combination of ~13 μm random and ~ 1 μm systematic errors in a strip pitch (5 mm). These included the errors of the measurements themselves. Even this level of precision seems to be almost acceptable (it would be equivalent to 1.3% calibration error), although it is definitely a very pessimistic estimation: this error could be well dominated by measurement errors and, also, the errors could be better for a smaller range needed for mini-strips (3 cm, rather 0.5 m).

Further studies of the mechanical accuracy of G10 etching are to be conducted. Also, we intend to verify the whole idea of the proposed technique against experimental results. Reliability of the scheme, although it seems to be very high (the worst what could happen is a wire break -- a negligible chance for 200-300 μm wire), has to be examined. The further search for the wires with a minimum droop is also desirable.

4. Conclusions.

1. The axial+projective alignment in the Muon System:

- **Decreases the coverage losses by 4-5%**
  (naive four muon efficiency would be ~18% higher);

- **Ensures that each track has hits in at least 2 super layers;**

- **Saves number of chambers and channels**
  (factor 3/4 for the barrel middle super layer);

- **Makes all barrel chambers of the same length (3.5 m);**

- **Allows one to eliminate chamber droop;**

- **Simplifies the support structure;**

- **Provides a tool for the global alignment;**

2. In particular, the proposed realization with a stretched wire and mini-strips:

- Does not require an attachment of any alignment device and eliminates extra transfer points;

- Simalteniously gives measurements in two directions (r_φ and radial);

- Provides half mil accuracy (transverse direction) over ±5 mm range of displacements in two directions and over ±10 mrad range of tilts in two directions;

- Intrinsically has low sensitivity to systematic errors: required calibration accuracy is relaxed up to ~0.5-1%; 5% cross talks are absolutely acceptable;

- Potentially saves alignment money (intrinsic simplicity due to absence of any external system except a stretched wire);

- Has intrinsic radiation hardness.

5. Acknowledgments.

The author is grateful to G.Alexeev, Yu.Bonushkin, A.Golutvin, I.Golutvin, Yu.Kiryushin, G.Mitselmakher, L.Osborne, A.Ostapchuk and L.Rosenson for the fruitful discussions of the questions concerned. Special discussions with F.Nimblett, J.Paradiso and B.Wadsworth are appriciated very much.

References.

1. G.Mitselmakher and A.Ostapchuk, GEM note TN-92-202.
2. R.Sawicki, in GEM note TN-93-282.
3. "LSDT's for the GEM Muon System", GEM note TN-92-203.
4. J.Paradiso, GEM note TN-92-150.
5. A.Ostapchuk, in GEM note TN-92- ,
   further analysis is expected to be done.
6. According to J.Paradiso.
7. F.Nimblett, private conversation.
8. J.Paradiso, private conversation.
9. I.Golutvin, private conversation.
10. TEXTRON Specialty Materials.
11. S.Whitaker, in GEM note TN-92-218.
12. K.Lau, in GEM note TN-92--133.

Figure Captions.

Fig.1. Projective+Axial Alignment (lines represent alignment paths). Axial Alignment ties all super layer chamber into effectively one big "chamber". Projective Alignment at the extremes in θ works for this "chamber" (it should be mentioned that the axial alignment provides a lot of additional information to be used in the interpolation procedure).

Fig.2(a). The schematic which was used to calculate the coverage losses in case when the projective alignment lens is absent:
a - chamber dead zone, b - clearance for structures in the SL2.

Fig.2(b). The schematic which was used to calculate the coverage losses in case with a projective alignment lens:
a - chamber dead zone, D - lens diameter.

Fig.3. The baseline barrel geometry which has been used for the calculations of the coverage losses. Circles in the SL2 show the gaps leading to coverage losses when the axial alignment is assumed.

Fig.4. The new layout of chambers in SL2. It reduces number of chambers, decreases the coverage losses, ensures that each track has hits in at least 2 super layers. Also, all chambers are now of the same length.

Fig.5. The idea of how the axial alignment could be realized in application with CSC's. Each strip board has bands of tiny mini-strips sticking out of the chamber. A wire stretched over these mini-strips and carrying pulses generates an induced charge, a centroid of which showing the relative position of the wire and a chamber corner.

Fig.6(a). G10 board with mini-strips on it. The wire is stretched over these mini-strips.

Fig.6(b). The distributions of the induced charge (arbitrary units) for different wire positions over a strip board (heights).

Fig.7. The RMS of systematic errors in reconstruction of centroid with preamps and ADC's calibrated to 0.5% accuracy. H is a distance between the wire and a strip board (height).

Fig.8. The RMS of systematic errors in reconstruction of the distance between the wire and a strip board (height) with preamps and ADC's calibrated to 0.5% accuracy.H is a distance between the wire and a strip board (height).

Fig.9. Systematic errors in reconstruction of a wire transverse position due to skewing of the distribution when the wire (or chamber) is tilted in both directions.

Table 1. Loss of coverage due to gaps between muon chambers.

With a clearance for the projective alignment lenses.

	$\Delta\eta$	$\delta\eta/\Delta\eta$	$\Delta\cos\theta$	$\delta\cos\theta/\Delta\cos\theta$
BARREL	1.221	6.0%	0.7599	5.8%
END-CAP	1.061	4.9%	0.1002	4.5%
TOTAL	2.282	5.5%	0.8601	5.6%

Table 2. Loss of coverage due to gaps between muon chambers.

With a clearance for the support structures only.

	$\Delta\eta$	$\delta\eta/\Delta\eta$	$\Delta\cos\theta$	$\delta\cos\theta/\Delta\cos\theta$
BARREL	1.221	1.5%	0.7599	1.9%
END-CAP	1.061	3.3%	0.1002	3.0%
TOTAL	2.282	2.3%	0.8601	2.0%

Table 3. Loss of coverage due to gaps between muon chambers for the new layout.

With a clearance for the support structures only (NEW LAYOUT).

	$\Delta\eta$	$\delta\eta/\Delta\eta$	$\Delta\cos\theta$	$\delta\cos\theta/\Delta\cos\theta$
BARREL	1.221	1.1%	0.7599	1.4%
END-CAP	1.061	3.3%	0.1002	3.0%
TOTAL	2.282	2.1%	0.8601	1.6%

Table 4. Efficiencies to detect 2 and 4 independent muons uniformly distributed in 4π.

	2 muon efficiency	4 muon efficiency
Old Layout (projective alignment)	1.00	1.00
New Layout (projective+axial)	1.09	1.18
Old Layout / Staged	0.78	0.60
New Layout / Staged	0.85	0.73

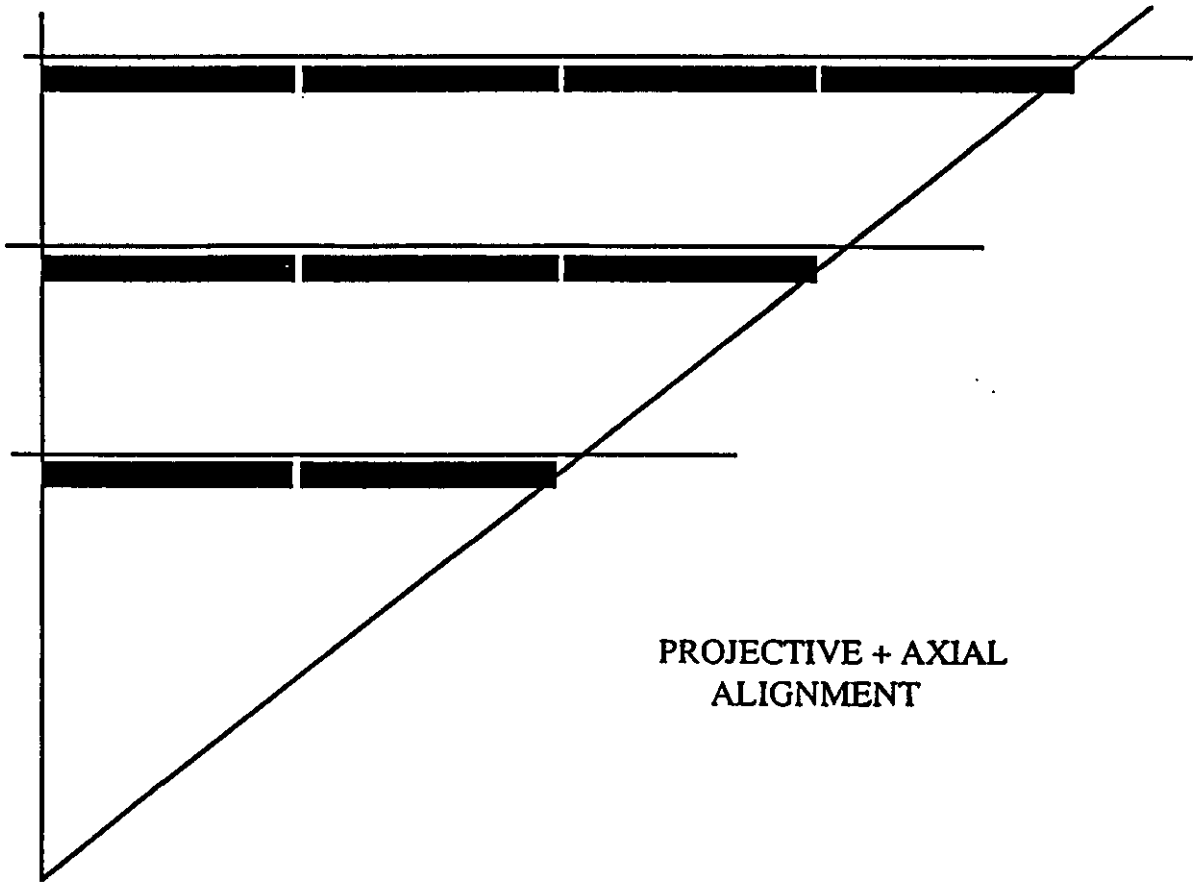

Fig. 1.

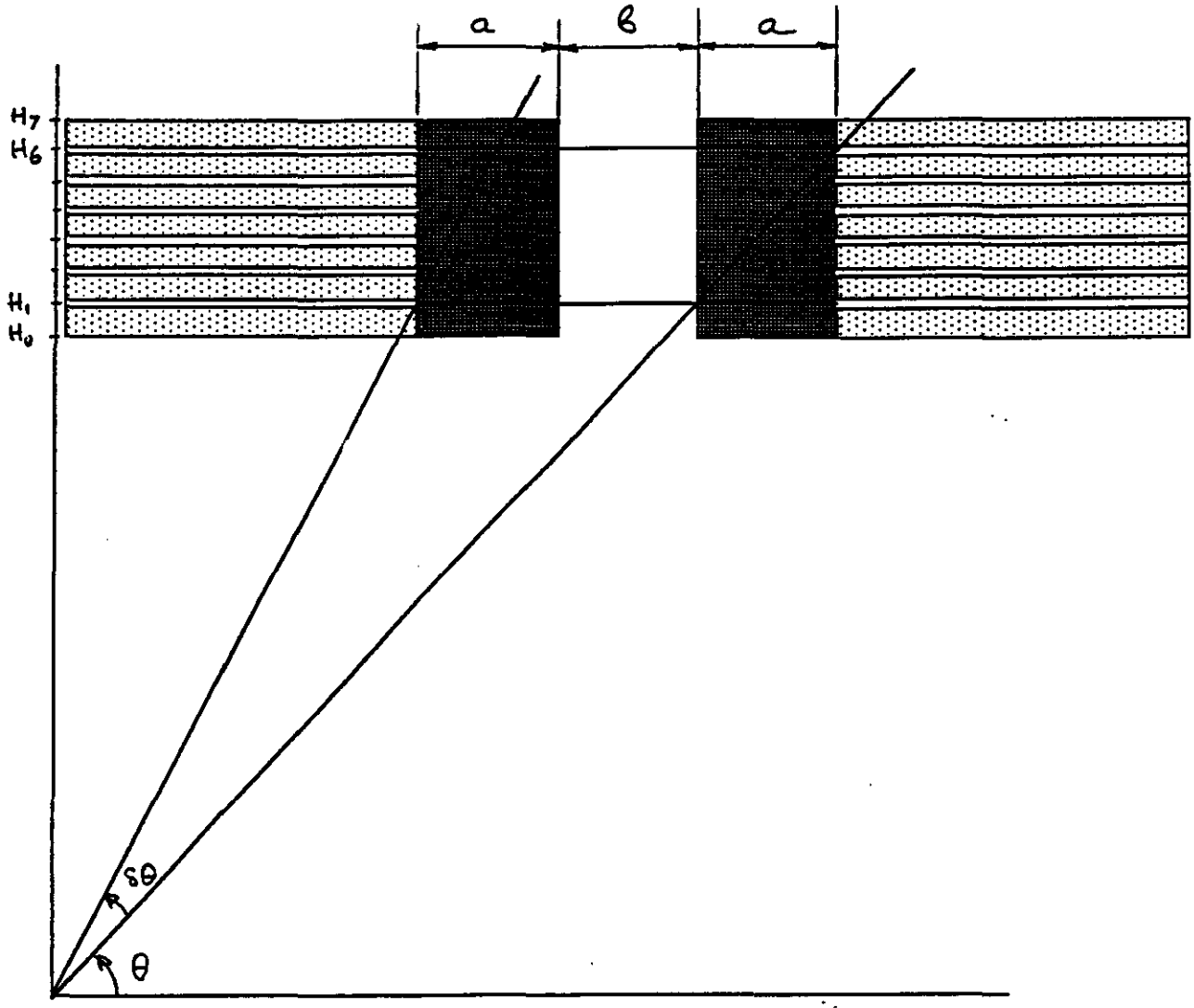

Fig. 2(a)

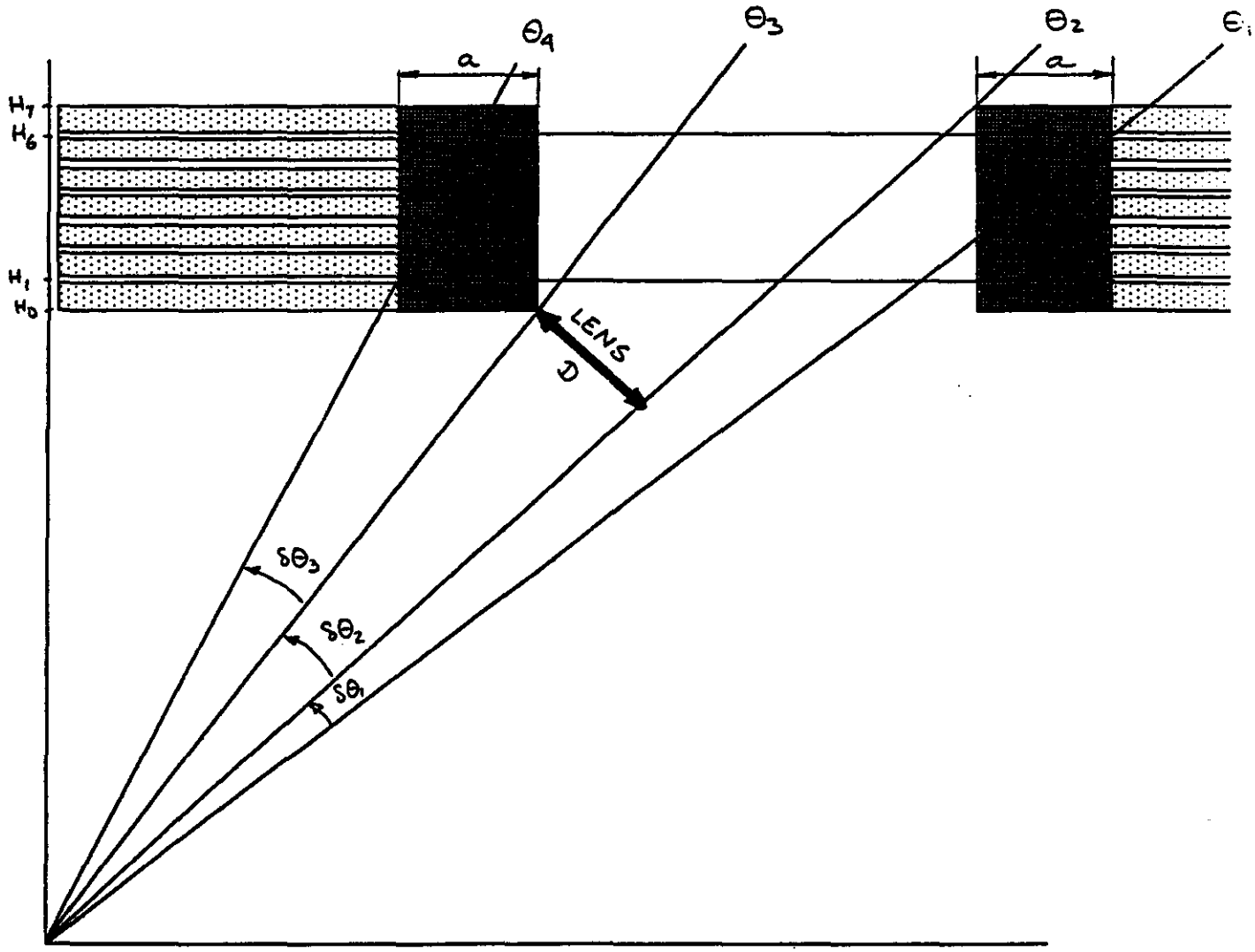
Θ_4
Θ_3
Θ_2
Θ_1
a
a
H_7
H_6
H_1
H_0
LENS
D
$\delta\Theta_3$
$\delta\Theta_2$
$\delta\Theta_1$

Fig. 2(b)

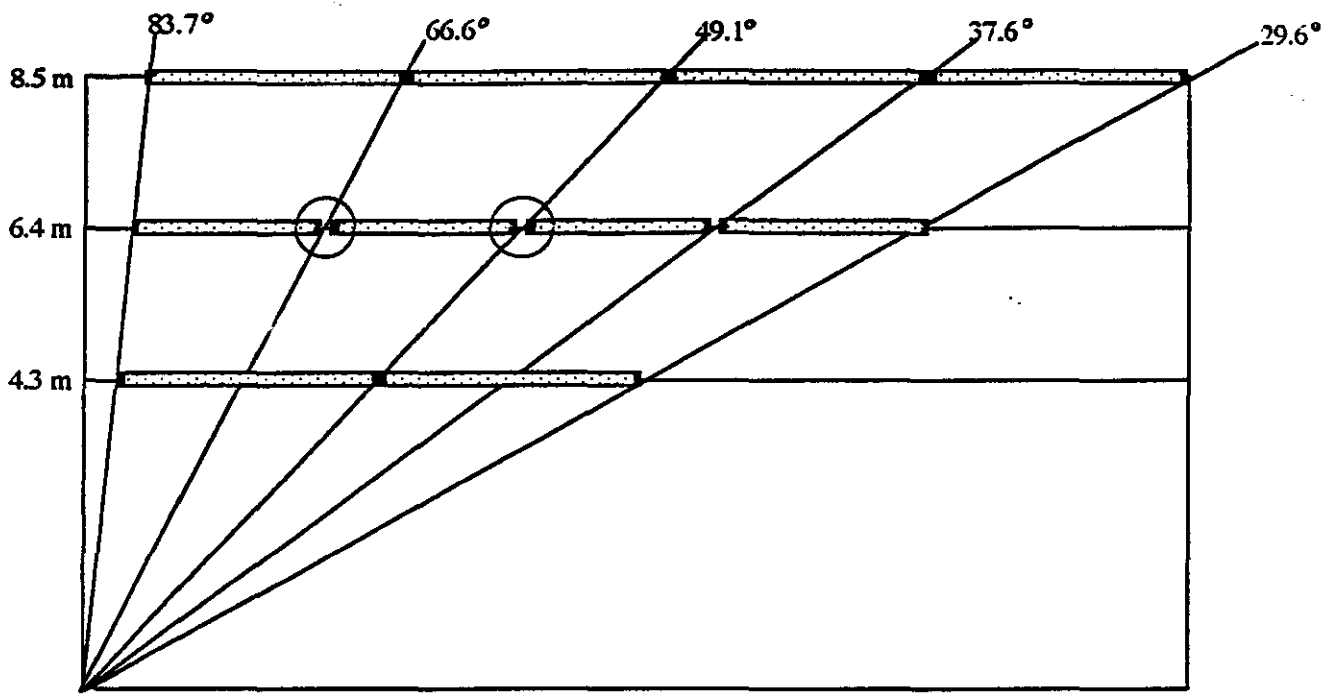

Fig. 3.

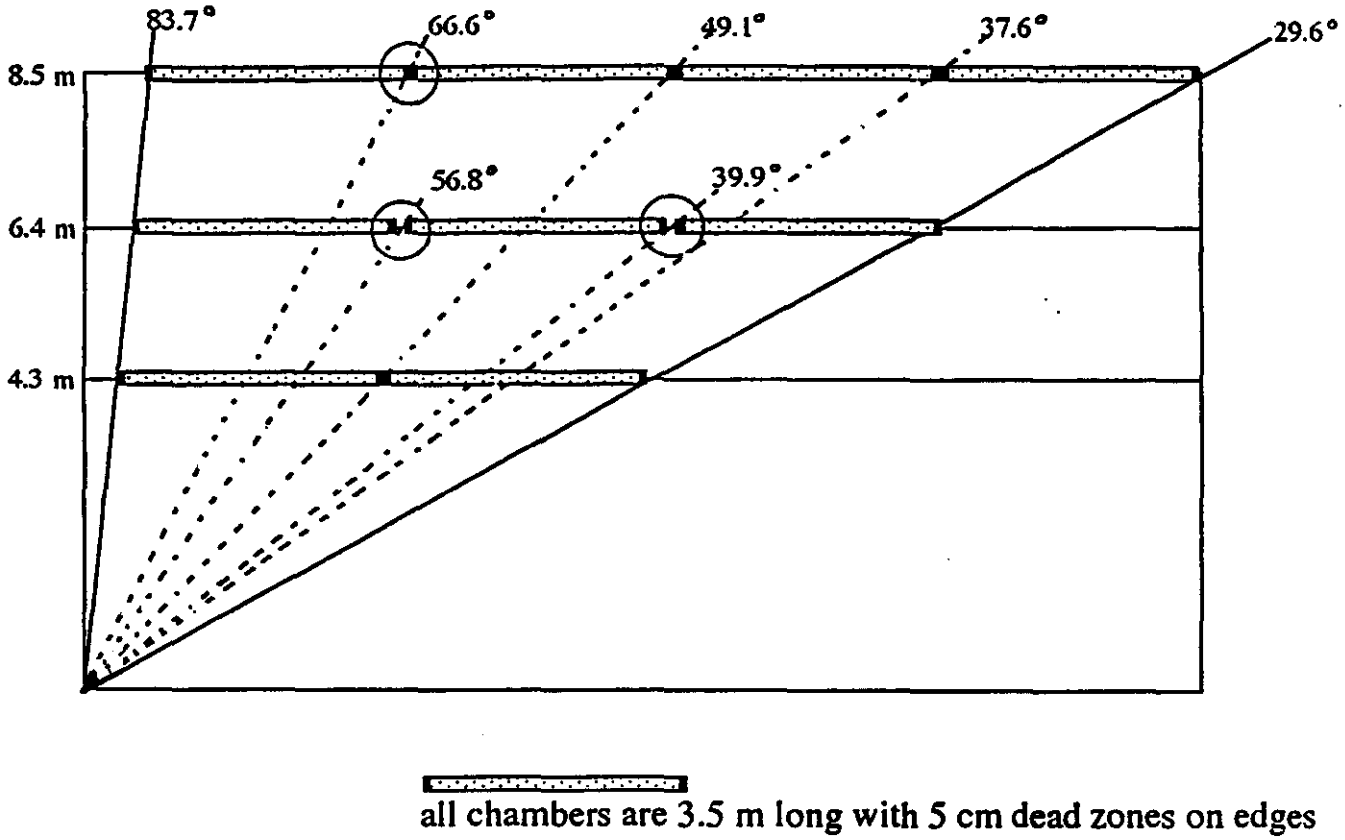
83.7°
66.6°
49.1°
37.6°
29.6°
8.5 m
56.8°
39.9°
6.4 m
4.3 m
all chambers are 3.5 m long with 5 cm dead zones on edges

Fig. 4.

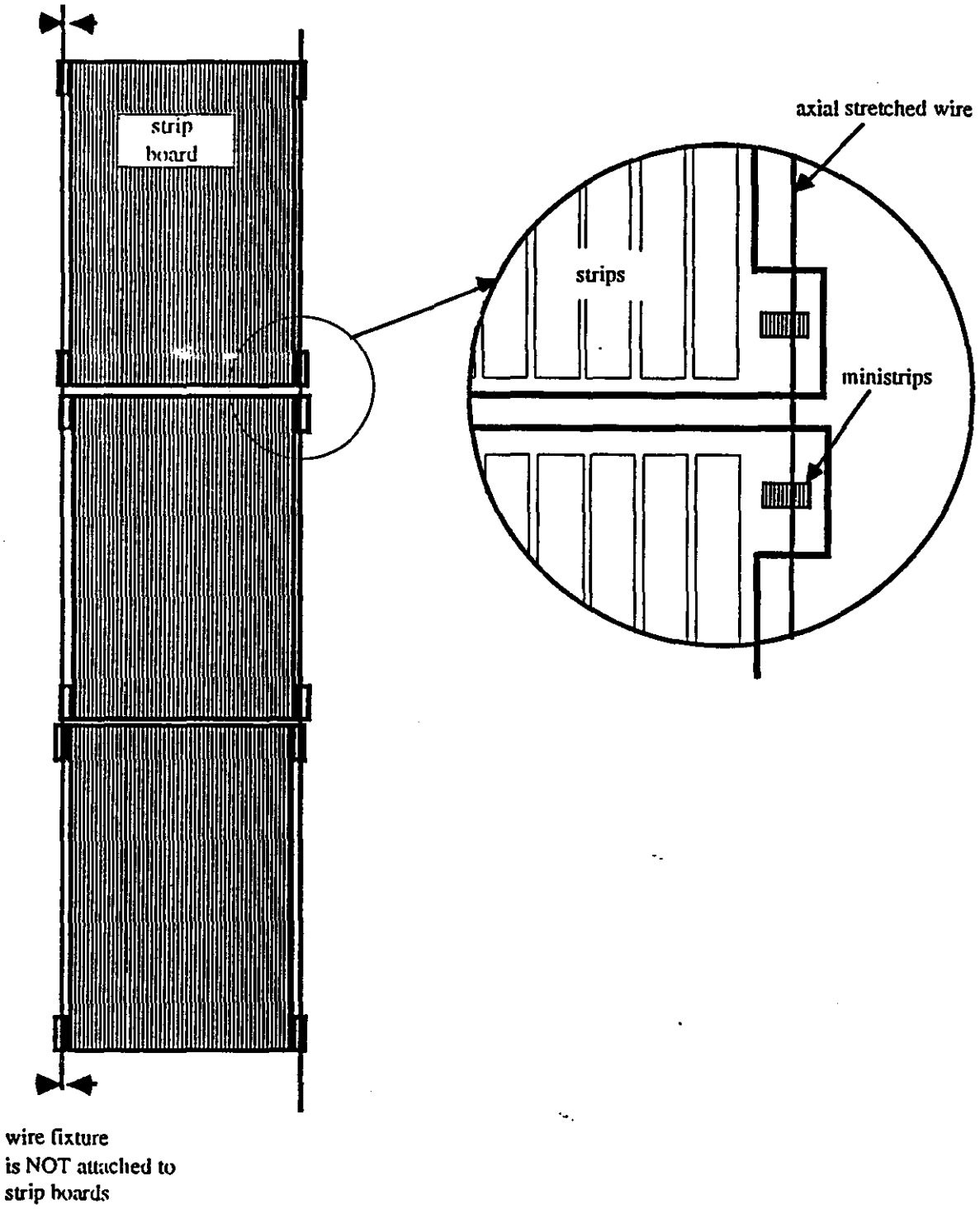
strip
board
axial stretched wire
strips
ministrips
wire fixture
is NOT attached to
strip boards

Fig. 5

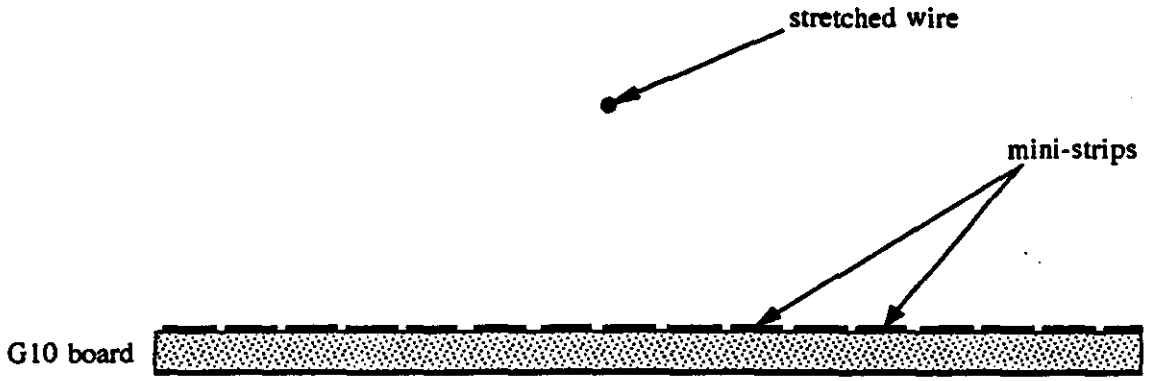

Fig. 6(a)

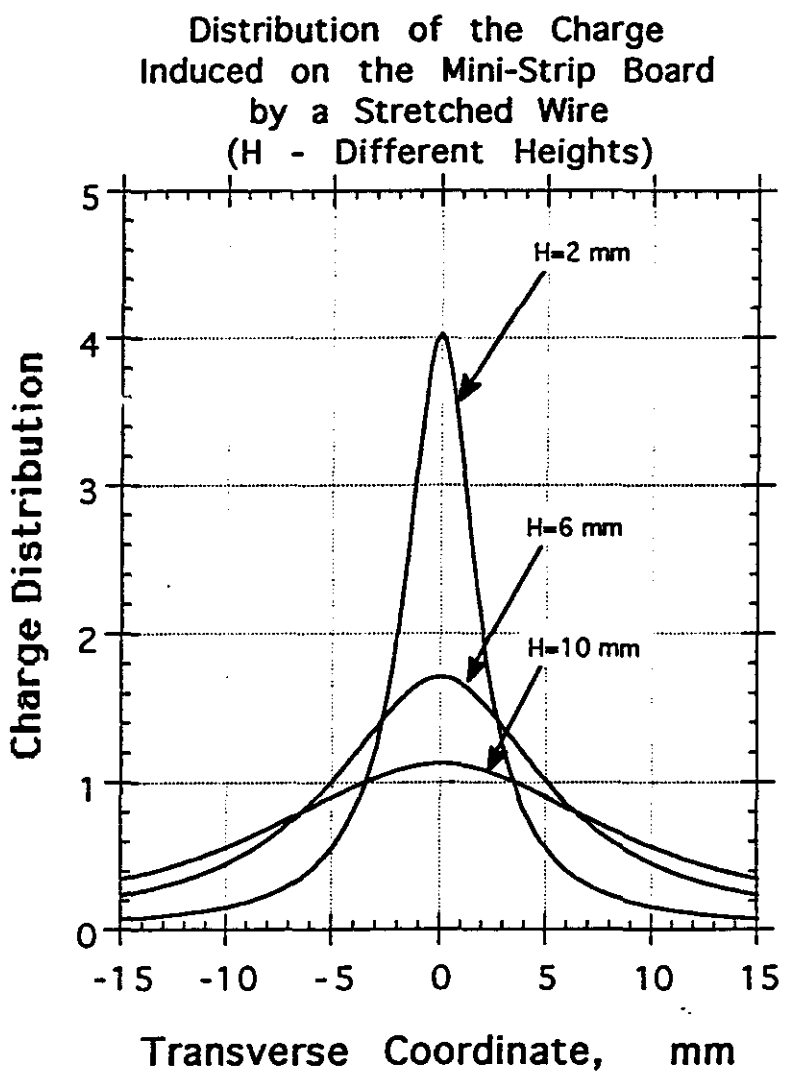
Distribution of the Charge
Induced on the Mini-Strip Board
by a Stretched Wire
(H - Different Heights)
H=2 mm
H=6 mm
H=10 mm
Charge Distribution
0
1
2
3
4
5
-15
-10
-5
0
5
10
15
Transverse Coordinate, mm

Fig. 6(b)

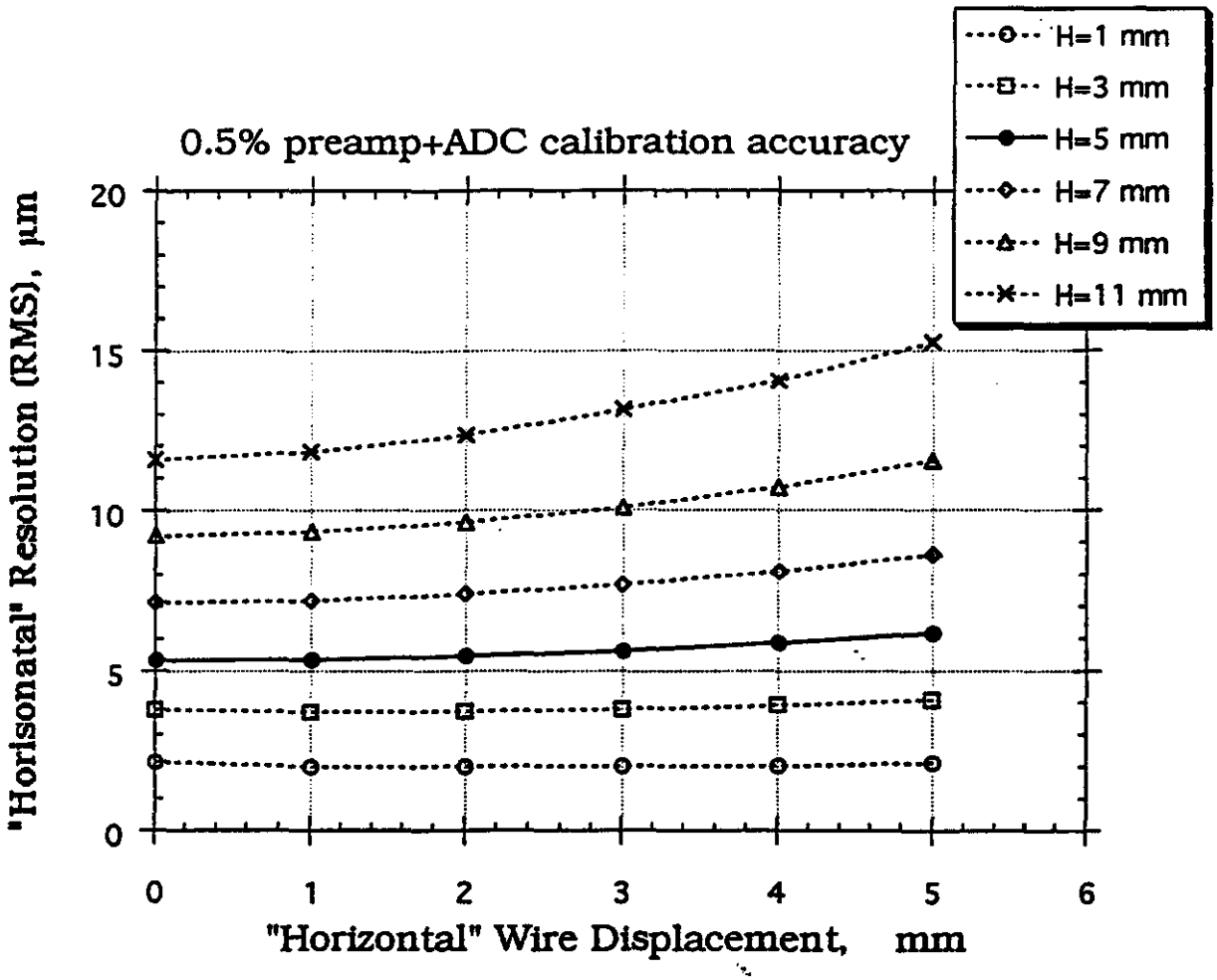
0.5% preamp+ADC calibration accuracy
H=1 mm
H=3 mm
H=5 mm
H=7 mm
H=9 mm
H=11 mm
"Horisonatal" Resolution (RMS), µm
20
15
10
5
0
0
1
2
3
4
5
6
"Horizontal" Wire Displacement, mm

Fig. 7

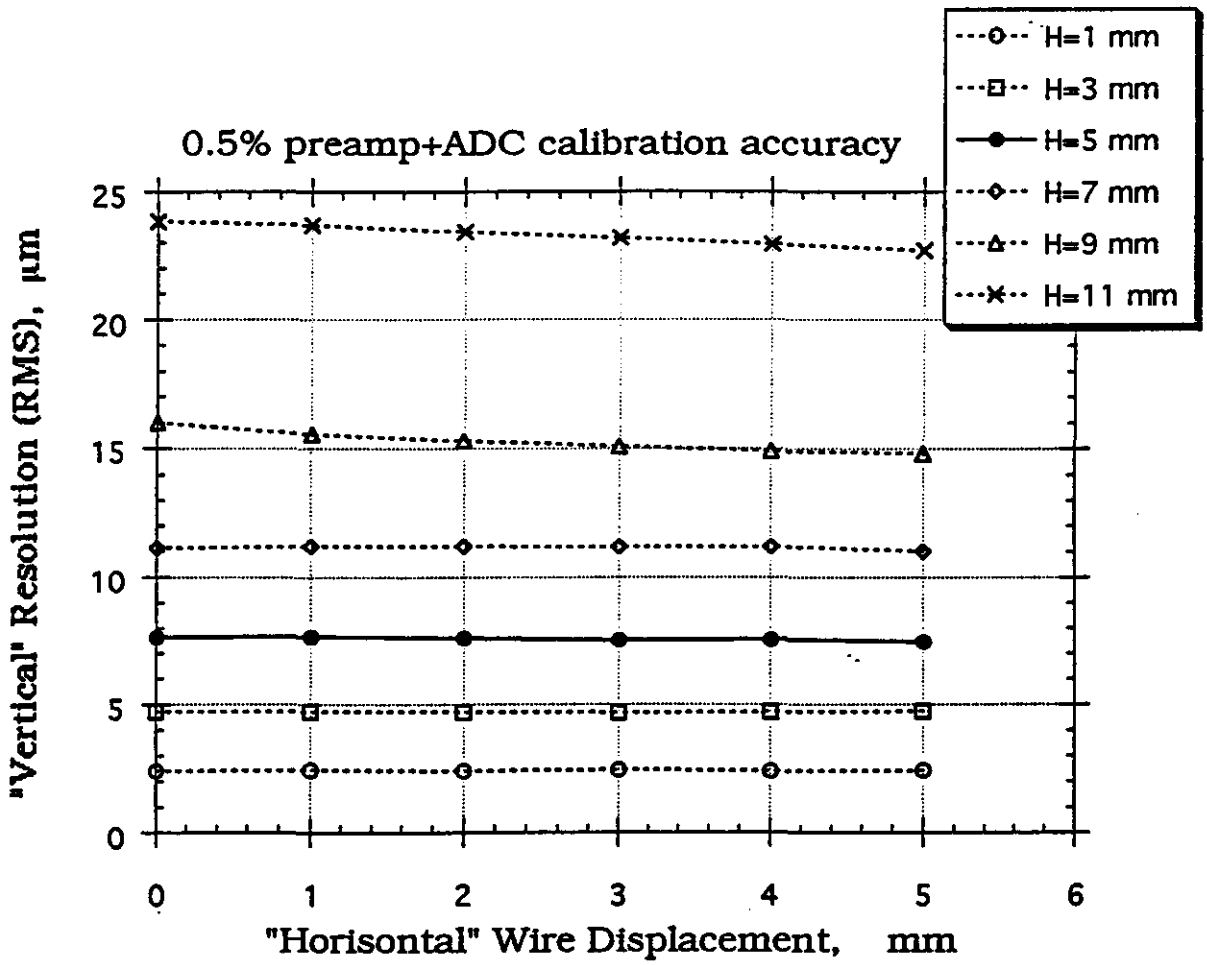
0.5% preamp+ADC calibration accuracy
H=1 mm
H=3 mm
H=5 mm
H=7 mm
H=9 mm
H=11 mm
"Vertical" Resolution (RMS), µm
25
20
15
10
5
0
0
1
2
3
4
5
6
"Horisontal" Wire Displacement, mm

Fig. 8

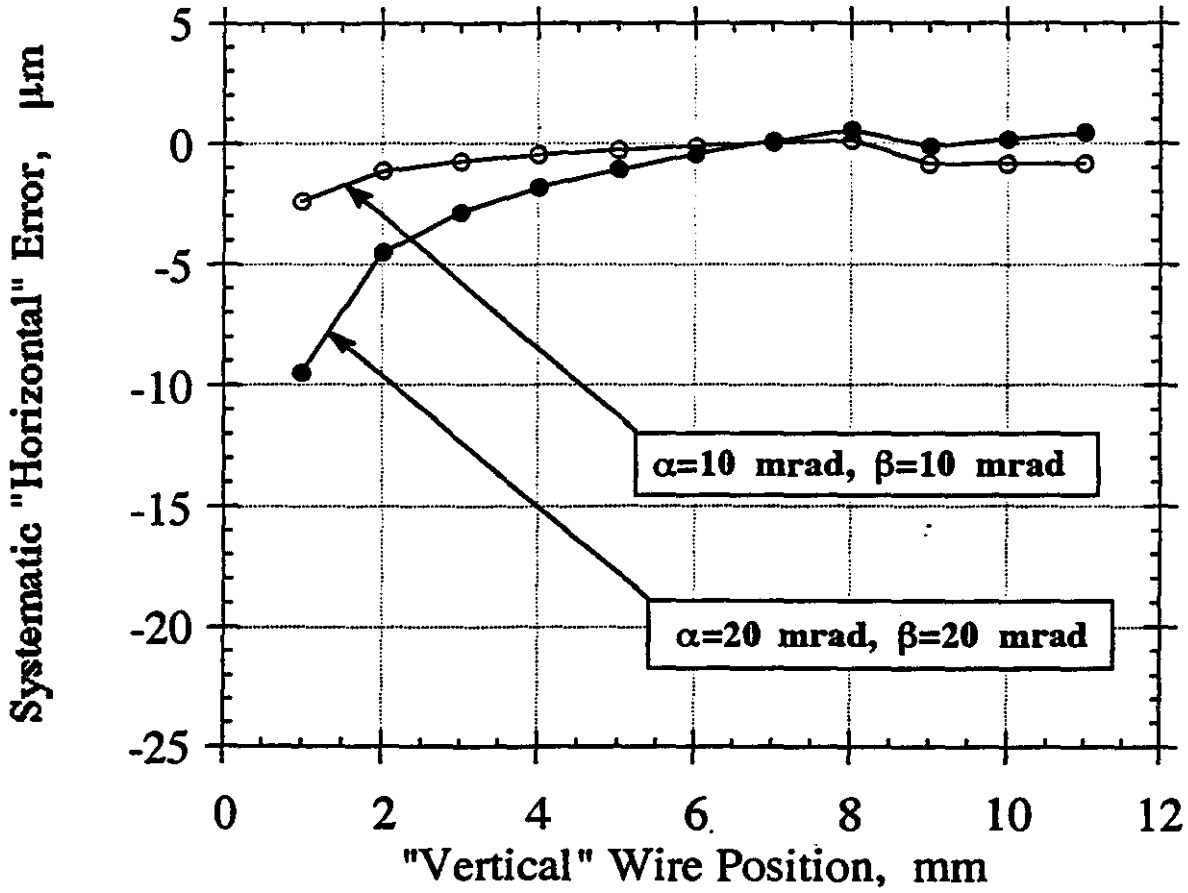
Systematic "Horizontal" Error, μm
5
0
-5
-10
-15
-20
-25
0
2
4
6
8
10
12
"Vertical" Wire Position, mm
α=10 mrad, β=10 mrad
α=20 mrad, β=20 mrad

Fig. 9

APPENDIX 1. CALCULATIONS OF COVERAGE LOSS (see fig. 2(a, b))

BARREL

NO LENS:

$$H_6 \operatorname{ctan}\theta - H_1 \operatorname{ctan}(\theta + \delta\theta) = a + b + a$$

$$H_6 \operatorname{ctan}\theta - H_1 \left(\operatorname{ctan}\theta - \frac{\delta\theta}{\sin^2\theta}\right) = a + b + a$$

$$\circledast \quad \delta\eta = \frac{\delta\theta}{\sin\theta} = \frac{2a+b}{H}\sin\theta - \frac{H_6 - H_1}{H}\cos\theta$$

WITH A CLEAR PATH for A LENS:

1)

$$H_6 \operatorname{ctan}\theta_1 - H_7 \operatorname{ctan}(\theta_1 + \delta\theta_1) = a$$

$$\frac{\delta\theta_1}{\sin\theta} = \frac{a}{H}\sin\theta + \frac{H_7 - H_6}{H}\cos\theta$$

2)

$$\delta\theta_2 = \frac{D}{H/\sin\theta}$$

$$\frac{\delta\theta_2}{\sin\theta} = \frac{D}{H}$$

3)

$$\frac{\delta\theta_3}{\sin\theta} = \frac{a}{H}\sin\theta + \frac{H_1 - H_0}{H}\cos\theta$$

$$\circledast \quad \delta\eta = \frac{\delta\theta}{\sin\theta} = \frac{D}{H} + \frac{2a}{H}\sin\theta + \frac{2(H_1 - H_0)}{H}\cos\theta$$

DIFFERENCE:

$$\Delta(\delta\eta) = \frac{D}{H} - \frac{b}{H}\sin\theta + \left(\frac{2(H_1 - H_0)}{H} + \frac{H_6 - H_1}{H}\right)\cos\theta$$

$$= \frac{D}{H} - \frac{b}{H}\sin\theta + \frac{H_7 - H_0}{H}\cos\theta$$

END-CAPS

No lens:

$$z_6 \tan(\theta + \delta\theta) - z_1 \tan\theta = a + b + a$$

$$\frac{\delta\theta}{\sin\theta} = \frac{2a+b}{z}\frac{\cos^2\theta}{\sin\theta} - \frac{z_6 - z_1}{z}\cos\theta$$

With a clear path for a lens

1)

$$z_6 \tan(\theta_1 + \delta\theta_1) - z_7 \tan\theta_1 = a$$

$$\frac{\delta\theta_1}{\sin\theta} = \frac{a}{z}\frac{\cos^2\theta}{\sin\theta} + \frac{z_7 - z_6}{z}\cos\theta$$

2)

$$\delta\theta_2 = \frac{D}{z/\cos\theta}$$

$$\frac{\delta\theta_2}{\sin\theta} = \frac{D}{z}\frac{\cos\theta}{\sin\theta}$$

3)

$$\frac{\delta\theta_3}{\sin\theta} = \frac{a}{z}\frac{\cos^2\theta}{\sin\theta} + \frac{z_1 - z_0}{z}\cos\theta$$

$$\frac{\delta\theta}{\sin\theta} = \frac{2a}{z}\frac{\cos^2\theta}{\sin\theta} + \frac{D}{z}\frac{\cos\theta}{\sin\theta} + \frac{2(z_1 - z_0)}{z}\cos\theta$$